Journal of Pharmacological and Toxicological Methods 63 (2011) 196–204

Contents lists available at ScienceDirect

Journal of Pharmacological and Toxicological Methods

journal homepage: www.elsevier.com/locate/jpharmtox

Original article

Measurement of oxygen consumption by murine tissues *in vitro*

Mohammed T. Al Samri [a], Mariam Al Shamsi [b], Suhail Al-Salam [c], Farida Marzouqi [a], Aysha Al Mansouri [a], Suleiman Al-Hammadi [a], Ghazala Balhaj [a], Shaikha K.M. Al Dawaar [a], Ruqayya S.M.S. Al Hanjeri [a], Sheela Benedict [a], Manjusha Sudhadevi [c], Walter Conca [d], Harvey S. Penefsky [e], Abdul-Kader Souid [a,*]

[a] Department of Pediatrics, Faculty of Medicine and Health Sciences, United Arab Emirates University, Al Ain, Abu Dhabi, United Arab Emirates, 17666, UAE
[b] Department of Immunology, Faculty of Medicine and Health Sciences, United Arab Emirates University, Al Ain, Abu Dhabi, United Arab Emirates, 17666, UAE
[c] Department of Pathology, Faculty of Medicine and Health Sciences, United Arab Emirates University, Al Ain, Abu Dhabi, United Arab Emirates, 17666, UAE
[d] Department of Internal Medicine, Faculty of Medicine and Health Sciences, United Arab Emirates University, Al Ain, Abu Dhabi, United Arab Emirates, 17666, UAE
[e] Department of Biochemistry, Public Health Research Institute, 225 Warren Street, Newark, New Jersey 07103

ARTICLE INFO

Article history:
Received 18 July 2010
Accepted 19 October 2010

Keywords:
In vitro
Cytotoxicity
Bioenergetics

ABSTRACT

Introduction: A novel *in vitro* system was developed to measure O_2 consumption by murine tissues over several hours. **Methods:** Tissue specimens (7–35 mg) excised from male Balb/c mice were immediately immersed in ice-cold Krebs–Henseleit buffer, saturated with 95% O_2:5% CO_2. The specimens were incubated at 37 °C in the buffer, continuously gassed with O_2:CO_2 (95:5). [O_2] was determined as a function of time from the phosphorescence decay rates ($1/\tau$) of Pd(II) meso-tetra-(4-sulfonatophenyl)-tetrabenzoporphyrin. The values of $1/\tau$ were linear with [O_2]: $1/\tau = 1/\tau o + kq\ [O_2]$; $1/\tau o$ = the decay rate for zero O_2, kq = the rate constant in $s^{-1}\ \mu M^{-1}$. **Results:** NaCN inhibited O_2 consumption, confirming oxidation occurred in the mitochondrial respiratory chain. The rate of respiration in lung specimens incubated in vitro for $3.9 \le t \le 12.4$ h was $0.24 \pm 0.03\ \mu M\ O_2\ min^{-1}\ mg^{-1}$ (mean ± SD, $n = 28$). The corresponding rate for the liver was 0.27 ± 0.13 ($n = 11$, $t \le 4.7$ h), spleen 0.28 ± 0.07 ($n = 10$, $t \le 5$ h), kidney 0.34 ± 0.12 ($n = 7$, $t \le 5$ h) and pancreas 0.35 ± 0.09 ($n = 10$, $t \le 4$ h). Normal tissue histology at hour 5 was confirmed by light and electron microscopy. There was negligible number of apoptotic cells by caspase 3 staining. **Discussion:** This approach allows accurate assessment of tissue bioenergetics *in vitro*.

1. Introduction

Many toxins directly or indirectly impair mitochondrial function. Therefore, in vitro measures of mitochondrial O_2 consumption (cellular respiration) are unmet needs. The phosphorescence O_2 analyzer (Lo, Koch, & Wilson, 1996) was recently utilized to monitor respiration in peripheral blood mononuclear cells (Shaban, Marzouqi, Al Mansouri, Penefsky, & Souid, 2010; Souid, Tacka, Galvan, & Penefsky, 2003). The method was subsequently utilized to monitored respiration in malignant cell lines (Tao, Ahmad, Penefsky, Goodisman, & Souid, 2006; Tao, Goodisman, Penefsky, & Souid, 2007). This novel approach accurately described the pharmacodynamics (sensitivity to drugs, dosing, time profile and mechanism of action) of various cytotoxic agents (e.g., doxorubicin, dactinomycin and platinum compounds). However, it was applicable only to cells in suspension.

Doxorubicin, an anthracycline antibiotic, is a widely used anticancer agent. The drug is known to intercalate with DNA and produce DNA breaks, primarily by stimulating topoisomerase II cleavable complex formation (Zunino & Capranico, 1990). It also induces accumulation of the P53 tumor suppressor protein, which causes cell cycle arrest. Moreover, it directly targets the mitochondria, impairing cellular respiration (Davis & Doroshow, 1986). Other cellular targets include the sarcoplasmic reticulum, which disturbs intracellular Ca^{2+} homeostasis. In the cell, the quinone moiety of doxorubicin-Fe(III) is reduced to semiquinone radicals, generating reactive oxygen species, which directly damage cell organelles (Doroshow, 1983). The outcome of these events is cell death, primarily by apoptosis (Bellarosa et al., 2001).

Measurements on O_2 consumption by fresh murine tissues are presented here. The purpose of this work was to describe an in vitro system that could be utilized for accurate monitoring of toxin-induced impairments of tissue bioenergetics, especially mechanism of action and dependence on exposure time and dosing.

Cells consume O_2 at a constant rate (zero-order kinetics). Thus, in vessels sealed from air, O_2 concentration in solutions containing cells or tissue specimens and glucose (as a respiratory substrate) declines linearly with time. Therefore, the rate of respiration is the negative of the slope of a plot of [O_2] vs. time.

A technique of monitoring respiration in various murine tissues in vitro over several hours is described. The results demonstrate stability of the tissue bioenergetics in vitro. This novel method permits expedient investigation of the effects of toxins on tissue respiration.

* Corresponding author. Tel.: +971 3 713 7429; fax: +971 3 767 2022.
E-mail address: asouid@uaeu.ac.ae (A.-K. Souid).

1056-8719/$ – see front matter © 2010 Elsevier Inc. All rights reserved.
doi:10.1016/j.vascn.2010.10.002

2. Materials and methods

2.1. Materials

Pd (II) complex of meso-tetra-(4-sulfonatophenyl)-tetrabenzo-porphyrin, sodium salt (Pd phosphor) was obtained from Porphyrin Products (Logan, UT). Complete® protease inhibitor cocktail was obtained from Roche Applied Science (Indianapolis, IN); this proprietary mixture inhibits serine, cysteine and metallo-proteases as well as calpains. Bovine serum albumin (free of endotoxins and fatty acids) and remaining reagents were obtained from Sigma-Aldrich (St. Louis, MO). Doxorubicin HCl (3.45 mM) was purchased from GensiaSicor Pharmaceuticals. Dactinomycin (actinomycin D, m.w. 1255.43) was purchased from Merck (Whitehouse Station, NJ).

2.2. Solutions

Pd phosphor (2.5 mg/ml = 2.0 mM) was prepared in dH_2O and stored at −20 °C. NaCN (1.0 M) was prepared in dH_2O and the pH was adjusted to ~7.0 with 12 N HCl. Antimycin (10 mg/mL), rotenone (0.1 M) and protonophore carbonyl cyanide *p*-(trifluoromethoxy) phenylhydrazone (FCCP, 0.1 M) were dissolved in absolute ethanol and stored at −20 °C. Glucose oxidase (10 mg/mL) was prepared in dH_2O and stored at −20 °C. One tablet of Complete® protease inhibitor cocktail was dissolved in 1.0 mL dH_2O (Water-For Injection) and stored at −20 °C. Dactinomycin solution was made fresh in dH_2O; its final concentration was determined by absorbance at 440 nm using an extinction coefficient of 24,450 M^{-1} cm^{-1} (Tao et al., 2006).

2.3. Tissues

Male *Balb/c* mice were anesthetized using urethane (100 μL/10 g body weight, using a 25% solution, w/v, in 0.9% NaCl). Samples (7–35 mg each) were excised from the tissues, using special scissors (Moria Vannas Wolg Spring, cat. ST15024-10). Tissue cuts were performed while the organ is still attached to the animal. Vertical cuts were usually made first, followed by horizontal cuts to collect the pieces. The specimens were immediately immersed in ice-cold Krebs-Henseleit buffer (115 mM NaCL, 25 mM $NaHCO_3$, 1.23 mM NaH_2PO_4, 1.2 mM Na_2SO_4, 5.9 mM KCL, 1.25 mM $CaCl_2$, 1.18 mM $MgCl_2$ and 6 mM glucose, pH ~7.4) saturated with 95% O_2:5% CO_2.

2.4. In vitro incubation

The tissue specimens were incubated at 37 °C (placed in 250 mL beakers in a circulating water bath) in 100 mL Krebs–Henseleit buffer with continuous gassing with 95% O_2:5% CO_2, without agitation. The pancreatic tissues were processed and incubated in the presence of Complete® protease inhibitors (2.0 μL/mL).

2.5. Oxygen measurement

The phosphorescence oxygen analyzer was used to measure respiration (Al Shamsi et al., 2010; Lo et al., 1996; Souid et al., 2003). At indicated time periods, specimens were removed from the incubation solution and placed in vials containing 1-ml Pd phosphor solution (air-saturated Krebs–Henseleit buffer containing 0.5% albumin and 3 μM Pd phosphor) for O_2 measurement at 37 °C. The Pd phosphor solution was freshly made, kept on ice and warmed to 25 °C prior to use. The vials were sealed with crimp top aluminum seals. Mixing was with the aid of a parylene-coated stirring bar (1.67 × 2.01 × 4.80 mm; V&P Scientific, Inc., San Diego, CA). The rate of respiration (μM O_2 min^{-1}) was set as the negative of the slope of a plot of [O_2] vs. time. Addition of 10 mM NaCN caused d[O_2]/d*t* to decrease almost to zero, confirming the decline in [O_2] with time was mainly due to mitochondrial O_2 consumption. Addition of glucose oxidase depleted the remaining O_2 in the solution. The change in [O_2] over ~3.5 h without tissues (drift rate) was <5% of the signal.

O_2 was detected using the Pd phosphor, which had an absorption maximum at 625 nm and a phosphorescence-emission maximum at 800 nm (Lo et al., 1996). The samples were exposed to light flashes (600/min) from a pulsed light-emitting diode array with peak output at 625 nm (OTL630A-5-10-66-E, Opto Technology, Inc), Wheeling, IL. Emitted phosphorescent light was detected by a Hamamatsu photo-multiplier tube (928) after first passing it through a wide-band interference filter centered at 800 nm. The amplified phosphorescence decay was digitized at 1.0 MHz by a 20-MHz A/D converter (Computer Boards, Inc.).

A program was developed using Microsoft Visual Basic 6, Microsoft Access Database 2007, and Universal Library components (Universal Library for Measurements Computing Devices, http://www.mccdaq.com/daq-software/universal-library.aspx). It allowed direct reading from the PCI-DAS 4020/12 I/O Board (PCI-DAS 4020/12 I/O Board, http://www.mccdaq.com/pci-data-acquisition/PCI-DAS4020-12.aspx). The software included relational database that stores experiments, pulses and pulse metadata, including slopes. Pulse detection was accomplished by searching for 10 phosphorescence intensities greater than 1.0 V (by default). Peak detection was accomplished by searching for the highest 10 data points of a pulse and choosing the data point closest to the pulse decay curve from the 10 highest data points of a pulse. Depending on the sample rate, a minimum number of data points per pulse was set and used as a cutoff to remove invalid pulses with too few data points (Shaban et al., 2010).

The main advantages of the developed software program over commercially available packages (e.g., DASY*Lab*™ or TracerDAQ™) are provision of full control and customization of data acquisition, storage and analysis. The choices of Visual Basic 6 and Access Database as programming and storage environments are due to their availability, simplicity, widespread use (which makes finding software developers less of a problem) and Visual Basic 6 components that read directly from the PCI card.

The phosphorescence decay rate ($1/\tau$) was characterized by a single exponential; $I = Ae^{-t/\tau}$, where I = Pd phosphor phosphorescence intensity. The phosphorescence decay rates ($1/\tau$) for β-glucose = 0 (air-saturated solution) was 0.0191/μs, for β-glucose = 125 μM 0.0057/μs, and for β-glucose = 500 μM ($1/\tau_o$, oxygen-depleted solution) 0.0028/μs. The corresponding lifetimes (τ) were 52 μs, 177 μs, and 352 μs, respectively.

The values of $1/\tau$ were linear with dissolved O_2 concentration: $1/\tau = 1/\tau^o + k_q[O_2]$, where $1/\tau$ = the phosphorescence decay rate in the presence of O_2, $1/\tau^o$ = the phosphorescence decay rate in the absence of O_2, and k_q = the second-order O_2 quenching rate constant in s^{-1} μM^{-1} (Lo et al., 1996).

Dissolved O_2 is expressed in mm Hg, mL O_2/L, mg O_2/L, or μmol/L (μM). For conversion:

A partial pressure of oxygen (PO_2) of 1.0 mm Hg = 0.03 mL O_2/L

$$1.0\ \mathrm{mL O_2/L} = 1.4276\ \mathrm{mg O_2/L}$$

$$1.0\ \mathrm{mg O_2/L} = 1000/32\ \mu\mathrm{M}$$

In freshwater at 760 mm Hg and 20 °C, the dissolved O_2 concentration is 9.1 mg/L, or 284 μM (Weiss, 1970). Using a Clark electrode, the PO_2 of the reaction mixture was 170.5 ± 6.6 mm Hg ($n = 4$), or 228 ± 9 μM. The 56 mm Hg difference between [O_2] in freshwater and the Pd solution reflects the effect of salinity on dissolved oxygen.

Two oxygen instruments were calibrated and used simultaneously. For calibration, the reaction contained buffer plus 3 μM Pd phosphor, 0.5% fat-free albumin, 50 μg/mL glucose oxidase and

various concentrations of β-glucose. To achieve a high signal-to-nose ratio throughout the entire range of [O_2], the photomultiplier tube was operated at 450 V for instrument A and at 500 V for instrument B. The value of k_q for instrument A was 101.1 $s^{-1}\mu M^{-1}$ and for instrument B 168.6 $s^{-1}\mu M^{-1}$. For instrument A, the value of $1/\tau$ for air-saturated solution (without glucose) was 28,330 s^{-1} (coefficient of variation, $C_v = 12\%$) and for O_2-depleted solution (with 500 μM β-glucose, $1/\tau_o$) 2875 s^{-1} ($C_v = 1\%$); the corresponding values for instrument B were 47,280 s^{-1} ($C_v = 11\%$) and 3241 s^{-1} ($C_v = 2\%$), respectively. The high values of C_v for the air-saturated solutions were due to the lower phosphorescence intensities with high [O_2] (little light reaching the photomultiplier tube). Oxygen concentration was calculated using, $1/\tau = 1/\tau^o + k_q[O_2]$.

2.6. Light microscopy

Samples of lung, liver, spleen, kidney and pancreas were fixed in 10% neutral formalin, dehydrated in increasing concentrations of ethanol, cleared with xylene and embedded in paraffin. Three-micrometersections were prepared from paraffin blocks and stained with haematoxylin and eosin.

Staining for apoptosis was performed using the avidin-biotin immunoperoxidase method to detect activated caspase 3 (Cell Signaling Technology, Boston, Massachusetts). The staining was performed on 5 μm paraffin sections, using rabbit anti-cleaved caspase 3 antibodies. Positive and negative control sections for apoptosis were used.

2.7. Electron microscopy

Samples were immersed in McDowell and Trump fixative for 3 h at 25 °C. Tissues were rinsed with phosphate buffer saline and fixed with 1% osmium tetroxide for 1 h. Samples were washed with dH_2O, dehydrated in graded ethanol and propylene oxide, infiltrated, embedded in Agar-100 epoxy resin and polymerized at 65°C for 24 h. Blocks were trimmed and semithin and ultrathin sections were cut with Reichert Ultracuts, ultramicrotome. The semithin sections (1 mm) were stained with 1% aqueous toluidine blue on glass slides. The ultrathin sections (95 nm) on 200 mesh Cu grids were contrasted with uranyl acetate followed by lead citrate double stain. The grids were examined and photographed under a Philips CM10 transmission electron microscope.

2.8. Lactate dehydrogenase (LDH)

The SYNCHRON® System was used to monitor the oxidation of L-lactate to pyruvate, with the concurrent reduction of β-nicotinamide adenine dinucleotide (NAD) to NADH. The reaction was monitored by the change in absorbance at 340 nm. The lowest limit of detection that distinguished signal from noise with 95% confidence was 5 IU/L (0.08 μkat/L).

3. Results

The rate of respiration of lung specimens (14–28 mg each), measured by the phosphorescence oxygen analyzer over 12-h period, was 0.25 ± 0.02 μM O_2 min^{-1} mg^{-1} (mean ± SD, $n = 28$), Fig. 1A. The results of six independent experiments over 3.9–12.4 h are shown in Fig. 1B. Addition of 100 μg/mL antimycin or 1.0 mM rotenone caused d[O_2]/dt to decrease by about 82% (Fig. 1C), confirming oxidation occurred in the mitochondrial respiratory chain. In three independent experiments, the rate of respiration (in μM O_2 min^{-1} mg^{-1}) in untreated lung tissue was 0.19 ± 0.04 and in lung tissue treated with 100 μg/mL antimycin 0.05 ± 0.01 or with 1.0 mM rotenone 0.07 ± 0.02.

Mitochondrial O_2 consumption by lung tissue exposed in vitro to 2 μM dactinomycin was measured over several hours (Fig. 1D). The purpose of this experiment was to show the method is applicable to studying effects of toxins on pneumatocyte bioenergetics. Tissue specimens excised from male *Balb/c* mice were immediately immersed in ice-cold Krebs–Henseleit buffer saturated with 95% O_2:5% CO_2. Specimens were incubated at 37 °C in the same buffer (as described in Methods) with and without 2 μM dactinomycin. At specific time points, specimens were placed in Krebs–Henseleit buffer containing 0.5% albumin and 3 μM Pd phosphor for O_2 measurement at 37 °C. The rate of respiration (in μM O_2 min^{-1} mg^{-1}) in untreated samples was 0.24 ± 0.04 ($n = 4$) and in treated samples 0.16 ± 0.02 ($n = 3$), $p < 0.05$.

Using the same method, uncoupler FCCP was shown to increase O_2 consumption by mitochondria isolated from Jurkat cells, but not by intact cells (Souid, Penefsky, Sadowitz, & Toms, 2006). Similarly, FCCP had no effect on O_2 consumption by intact murine tissues (personal observations). Using digitonin to permeabilize the cells, Dranger and Lehninger (1982) showed FCCP increased O_2 consumption by cytotoxic macrophage-injured L1210 cells. However, this treatment produces leakage of metabolic fuels, causing unreliable measurements of respiration. Nevertheless, O_2 consumption by lung tissue permeabilized with 0.005% digitonin was increased by 46% in the presence of 80 nM FCCP (Fig. 1E).

Fig. 2A shows representative experiment of liver tissue respiration (13–30 mg specimens) over ~5 h; the rate of respiration ($n = 4$) was 0.23 ± 0.05 μM O_2 min^{-1} mg^{-1}. Fig. 2B shows the results of three independent experiments over ~5 h period. Addition of 10 mM NaCN caused d[O_2]/dt to decrease to zero (Fig. 2C), confirming oxidation occurred in the mitochondrial respiratory chain. The addition of glucose oxidase caused rapid depletion of O_2 in the solution (Fig. 2C).

Table 1 summarizes all measurements on lung, liver, spleen, kidney and pancreatic tissues. The maximum durations of in vitro incubation of the tissues are also shown.

Mitochondrial O_2 consumption by murine tissues exposed in vitro to 10 μM doxorubicin was measured over several hours (Table 2). The results show that doxorubicin mildly inhibited pneumatocyte respiration, while hepatocyte and spleen cell respiration were unaffected (Table 2).

Fig. 3 shows the histology of lung, liver, spleen, kidney and pancreatic tissues incubated as described in Methods for 5 h. Normal architecture and histology were evident (Fig. 3, left panels). Only the spleen tissue showed a positive staining for caspase 3 (Fig. 3F). The haematoxylin and eosin sections showed normal cell morphology and tissue architecture. The presence of mitotic figures in the tissues further supported their viability and preservation of active processes (Fig. 3, left panels). In the lung, the alveolar spaces had uniform size and intact inter-alveolar septae. The relations between respiratory bronchioles, terminal bronchioles and interstitial blood vessels were also normal (Fig. 3A). In the liver, the hepatic plates had intact single cell layer configuration and normal relations with sinusoidal cells. The relation between terminal hepatic venules and portal tracts was also maintained (Fig. 3C). The pancreatic tissue showed normal exocrine pancreatic acini and normal islet cell morphology. It also showed normal architectural relations between the exocrine pancreatic acini and the islets of Langerhans (Fig. 3E). The kidney tissue showed normal morphology of the renal tubules and glomeruli and intact architectural relations between the renal glomeruli, tubules and interstitium (Fig. 3G). The splenic tissue showed normal lymphoid - cells, macrophages, leuckocyte polymorphs and endothelial cells; the architectural relation between the white and red pulp was also intact (Fig. 3I).

Fig. 4A–E shows transmission electron micrographs of the studied tissues. Overall, the ultrastructures of the cellular micro-organelles were well preserved in the lung (A), liver (B), kidney (C), pancreas (D) and spleen (E) specimens.

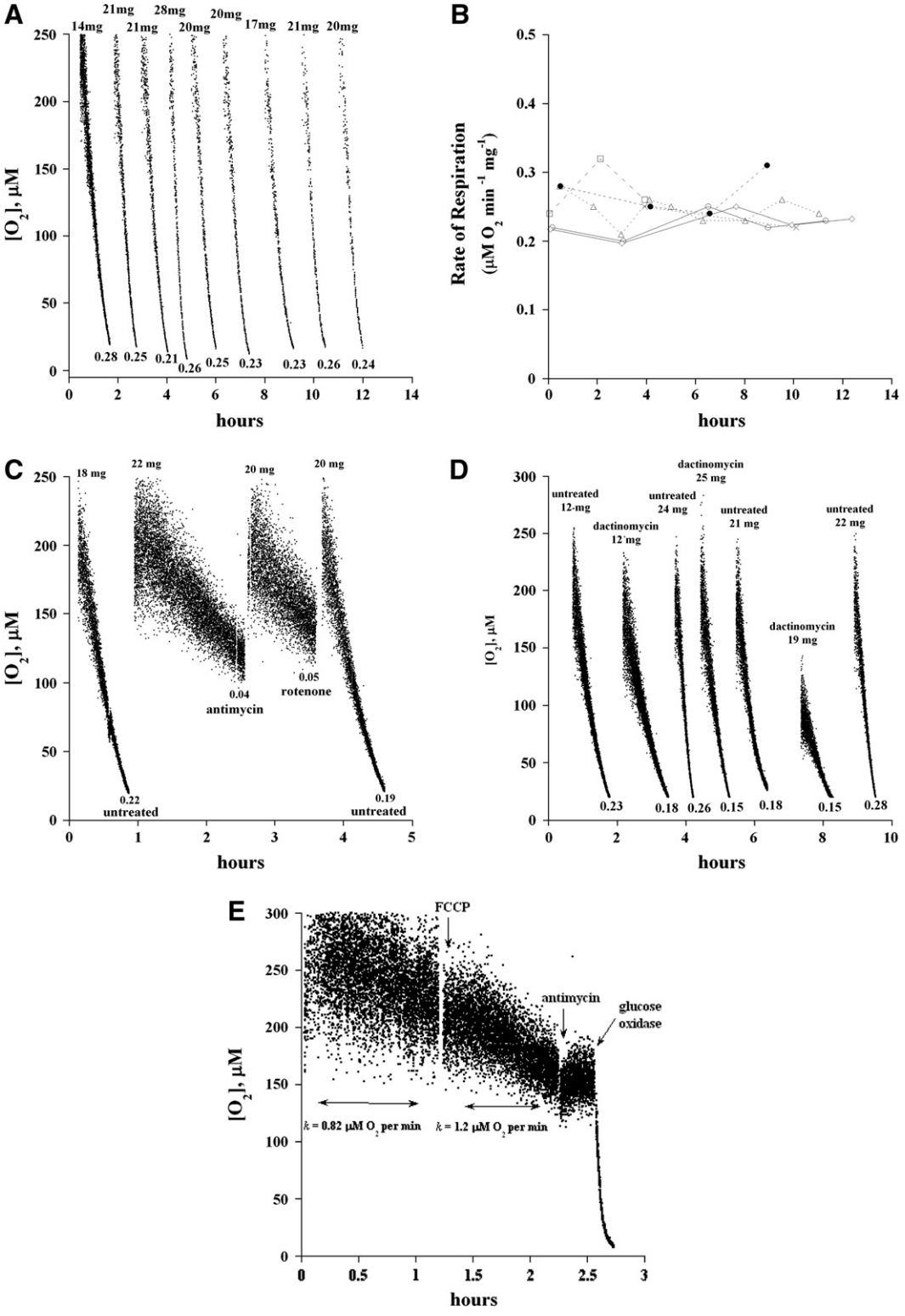

Fig. 1. Lung tissue respiration. (A) A representative experiment of O_2 consumption by lung tissue. Specimens were excised (14–28 mg each) from the lung of an anesthetized mouse and immediately immersed in ice-cold Krebs–Henseleit buffer saturated with 95% O_2:5% CO_2. The samples were incubated at 37 °C in the same buffer with continuous gassing with O_2:CO_2. At indicated time periods, specimens were removed from the incubation mixture, weighed and then placed in Krebs–Henseleit buffer containing 0.5% albumin and 3 μM Pd phosphor for O_2 measurement. The rate of respiration was set as the negative of the slope of [O_2] vs. time. The weight is shown at the top and the respiration rate (in μM O_2 min^{-1} mg^{-1}) at the bottom of each run. (B) Respiration rates (in μM O_2 min^{-1} mg^{-1}) of five independent experiments over 3.9–12.4 h periods. (C) O_2 consumption by lung tissue with and without 100 μg/mL antimycin or 1.0 mM rotenone. (D) O_2 consumption by lung tissue with and without 2 μM dactinomycin. (E) Effect of FCCP (80 nM) on O_2 consumption by lung tissue. O_2 consumption was measured in Krebs–Henseleit buffer containing 0.005% digitonin, 0.5% albumin and 3 μM Pd phosphor.

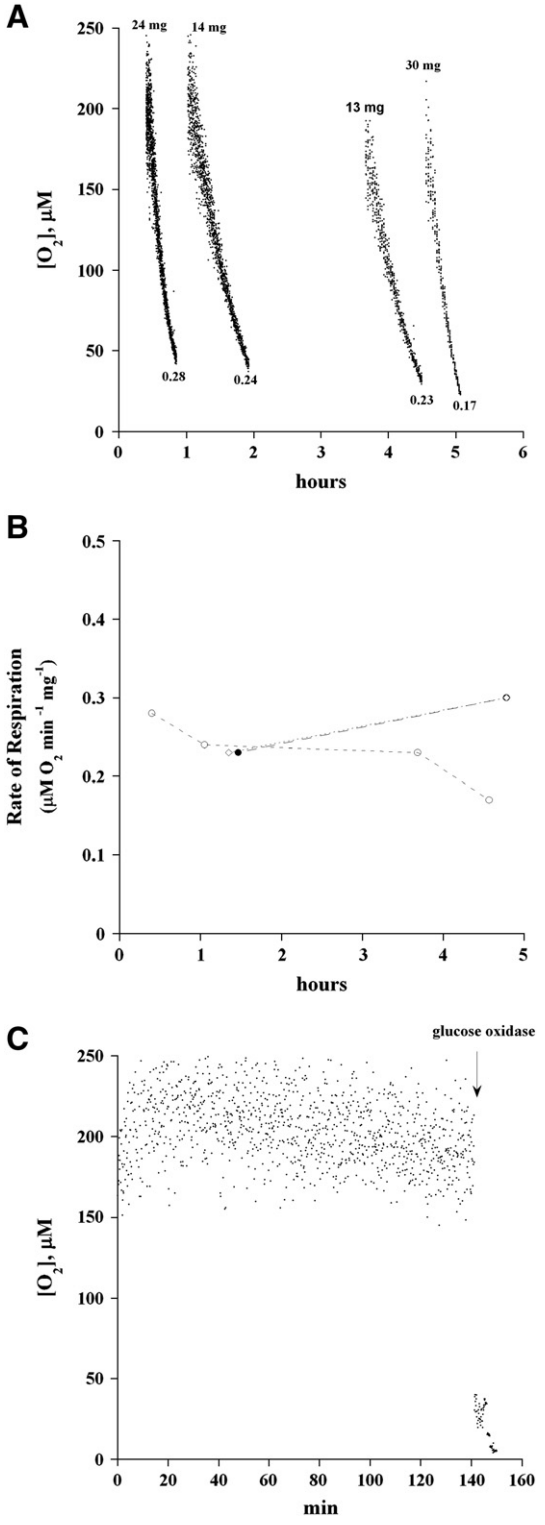

Fig. 2. Liver tissue respiration. (A) A representative experiment of O_2 consumption by liver tissue. Specimens were collected and processed as in legend to Fig. 1. The weight is shown at the top and the respiration rate (in μM O_2 min^{-1} mg^{-1}) at the bottom of each run. (B) Respiration rates (in μM O_2 min^{-1} mg^{-1}) of three independent experiments over ~5 h periods. (C) O_2 consumption by liver tissue in the presence of 10 mM NaCN.

LDH was measured (under the same conditions described above) in the incubation buffer that contained tissue specimens for 0, 3 and 6 h. In three independent experiments, the values of LDH were below the lowest limit of detection in all studied tissues.

Table 1
Measurements of O_2 consumption in murine tissues.

Tissue	Rate of respiration (μM O_2 min^{-1} mg^{-1})	Duration of in vitro incubation of the specimens
Lung[1]	0.24 ± 0.03 (28)	≤12.4 h
Liver[2]	0.27 ± 0.13 (11)	≤5.0 h
Spleen[2]	0.28 ± 0.07 (10)	≤5.0 h
Kidney[2]	0.34 ± 0.12 (7)	≤5.0 h
Pancreas[2]	0.35 ± 0.09 (10)	≤4.0 h

Values are mean ± SD (n = number of runs).
For unit conversion, 1.0 mL O_2 = 1.4276 mg or 0.0446125 mmol.
[1]Five independent experiments.
[2]Three independent experiments.

4. Discussion

The first technical advance arising from the current study is the way of maintaining viable tissues in vitro for several hours. The described procedure is relatively simple and requires minimum tissue handling. It allows comprehensive analyses (e.g., cellular respiration, histology and electron microscopy) in vitro over extended periods of time. One advantage of this approach is evading extensive tissue manipulation and collagenase digestion required for single cell preparation. However, a successful tissue collection method requires rapid (within 30 s) collection of thin (preferably less than 0.2 mm thick), small (preferably less than 20 mg weight) slices while the organ is still attached to the animal and well perfused. Drenching the thoracic or abdominal cavity with appropriate ice-cold, well-oxygenated (PO_2>400 mm Hg) buffer before the surgical procedure is recommended. The specimens should be immediately immersed in buffer supplemented with potent inhibitors of all potential proteases. It worth noting that some anti-proteases are less effective in the acid pH range (e.g., aspartic acid protease inhibitors) and addition of pepstatin may be necessary. Furthermore, in vitro gentle handling of all tissues is critical for maintaining viability for several hours, especially if incubation with drugs or toxins is necessary (Al Shamsi et al., 2010).

The second technical advance of this study is the feasibility of measuring respiration (cellular mitochondrial oxygen consumption) in various murine tissues over several hours. Our previous work on measuring cellular respiration was limited to cell suspensions, such as transformed cell lines and human peripheral blood mononuclear cells (Souid et al., 2003, Tao et al., 2006, 2007). The novel approach described here permits accurate estimation of tissue oxygen consumption in vitro over extended periods of time. The method allows investigating effects of toxins and drugs on tissue bioenergetics, as shown in Table 2 and Fig. 1C (Al Shamsi et al., 2010). It also permits reliable estimations of dosing, time course and mechanism of action (e.g., caspase-mediated cytotoxicity that can be blocked by the pan-caspase

Table 2
Measurements of O_2 consumption in murine tissues with and without doxorubicin.

Tissue	Rate of respiration (μM O_2 min^{-1} mg^{-1})		
	Untreated	Doxorubicin (10 μM)	
Lung[1]	0.22 ± 0.06 (10)	0.17 ± 0.03 (8)	p = 0.029
Liver[2]	0.20 ± 0.05 (10)	0.19 ± 0.05 (9)	p = 0.608
Spleen[3]	0.20 ± 0.04 (9)	0.20 ± 0.03 (8)	p = 0.942

Values are mean ± SD (n).
[1]Three independent experiments over 7.5–10 h.
[2]Three experiment over 5–6 h.
[3]Three independent experiments over 5–10 h.

inhibitor benzyloxycarbonyl-val-ala-DL-asp-fluoromethylketone) (Tao et al., 2006, 2007).

A significant contribution of this work is that cellular bioenergetics in murine tissues is stable in vitro over 4–12 h, depending on the type of tissue (Table 1). Thus, the assay is suitable for time-dependent organ toxicity studies, such as cytotoxic drugs and effects of environmental toxins on tissue respiration (Al Shamsi et al., 2010). Moreover, the method allows accurate monitoring of mitochondrial cell death during apoptosis (Ricci et al., 2004; Tao et al., 2006, 2007).

The described tissue processing is highly reproducible. As discussed above, the procedure does not involve extensive tissue manipulations, such as collagenase treatment. Therefore, the histology (Fig. 3, left panels) and micro-organelle ultrastructure (Fig. 4A–E) are well preserved. Caspase 3 staining was negative in all tissues; expect for the spleen (Fig. 3F). Cyanide (Fig. 2C), antimycin and rotenone (Fig. 1C) all inhibited O_2 consumption, confirming the oxidation occurred in the mitochondrial respiratory chain.

The term cellular respiration implies delivery of O_2 and metabolic fuels to the mitochondria, oxidation of reduced metabolic fuels with passage of electrons to O_2, and synthesis of ATP. Impaired respiration thus entails an interference with any of these processes. The effects of cytotoxic drugs on mitochondrial O_2 consumption by various malignant cell lines was recently reported (Al Shamsi et al., 2010;

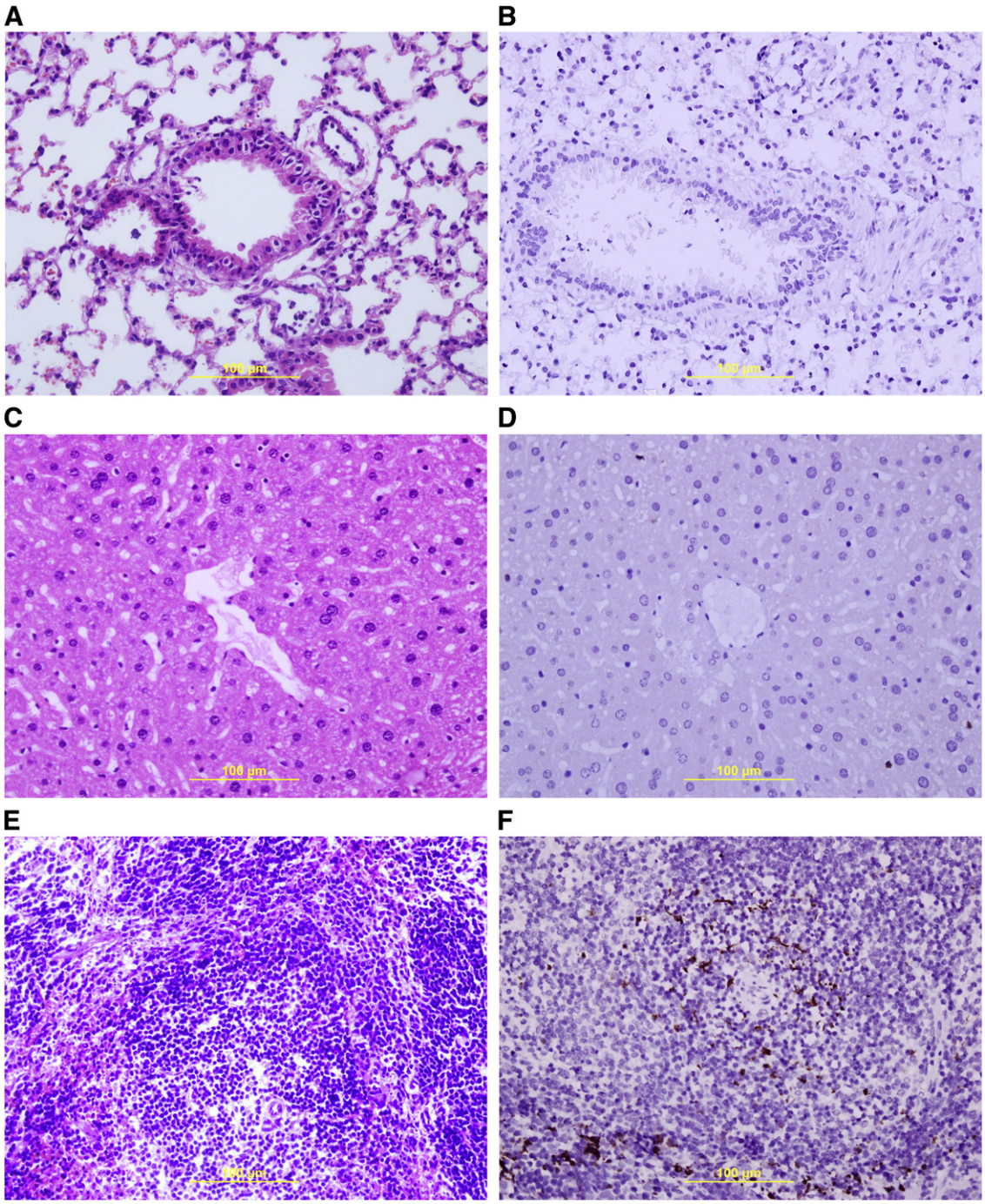

Fig. 3. Histology. Tissue samples were incubated in Krebs–Henseleit buffer at 37 °C for 5 h. The specimens were then stained with haematoxylin and eosin (left panels) or anti-cleaved caspase 3 antibodies (right panels). A-B, lung; C-D, liver; E-F, spleen; G-H, kidney; and I-J, pancreas.

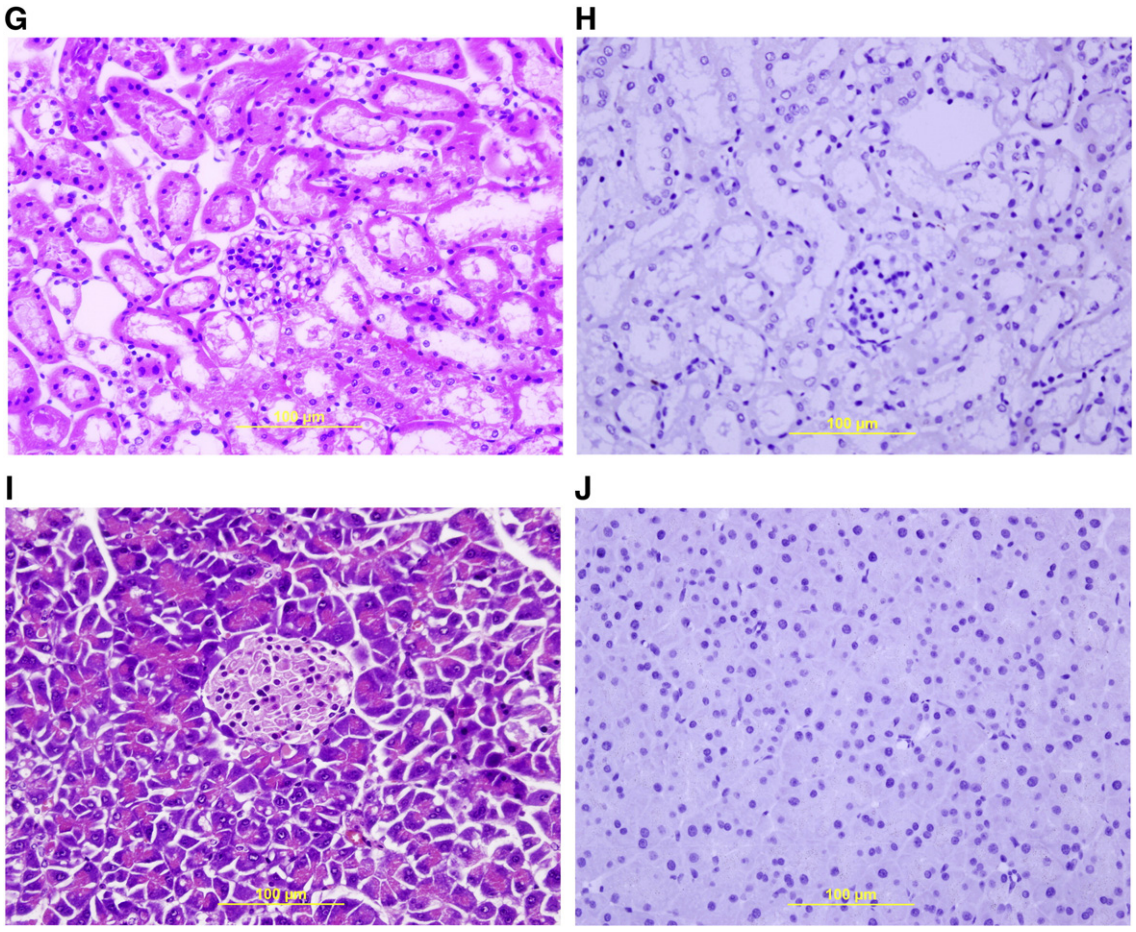

Fig. 3 (*continued*).

Shaban et al., 2010; Tao et al., 2006, 2007). This study shows reasonable in vitro stability of murine tissues, allowing reliable measurements of respiration over several hours (Table 1). It also shows feasibility of evaluating effects of cytotoxic agents (e.g., doxorubicin and dactinomycin) on cellular bioenergetics in fresh tissues (Table 2 and Fig. 1D).

Measurement of O_2 using Pd(II)-meso-tetra-(4-sulfonatophenyl)-tetrabenzoporphyrin (Pd phosphor) was first introduced by Wilson and colleagues (Lo et al., 1996). The detection is based on the principle that O_2 quenches the phosphorescence of Pd phosphor; thus, the observed phosphorescence is inversely related to O_2 concentration. This method was employed here to measure O_2 consumption by various murine tissues over several hours.

Respiration of lung specimens was stable in vitro for about 12 h (Fig. 1A and B). By contrast, the liver, spleen, kidney and pancreas were stable for periods ranging from 4 to 6 h. Stability of the pancreatic tissues improved with the addition of protease inhibitors. Nevertheless, the rates of respiration in studied lung, liver and spleen specimens were similar (Table 1). On the other hand, both kidney and pancreas showed similar rates of respiration, about 1/3 higher than the rest of the tissues (Table 1).

Vaupel, Fortmeyer, Runkel, and Kallinowski (1987) reported an in vitro rate of O_2 consumption by human breast cancer xenografts of 7.7–10.4 µL O_2 $min^{-1}g^{-1}$ (or 0.34–0.46 nmol O_2 $min^{-1}mg^{-1}$), which is similar to our findings in murine tissues (0.24-0.35 nmol O_2 $min^{-1}mg^{-1}$), Table 1. In vivo O_2 consumption by "normal" human kidneys is 5.5 ± 0.6 mL O_2 min^{-1} 100 g^{-1} (or ~2.45 nmol O_2 $min^{-1}mg^{-1}$) (Crosley, Castillo, & Rowe, 1961), a rate that is 7-fold higher than that seen in vitro with the mouse kidney (Table 1).

Oxygen consumption by cortical slices from Wistar Kyoto rat kidney was ~0.6 nmol $min^{-1}mg^{-1}$ (Adler & Huang, 2002). Whereas in a similar study by Deng et al. (2005) in Wistar rat kidneys, O_2 consumption rates were 1.22 nmol $min^{-1}mg^{-1}$ and 48.4 ± 6.3 nmol $min^{-1}mg^{-1}$ tissue protein.

In vitro O_2 consumption by rat liver was 5.6 ± 0.1 µL O_2 $min^{-1}mg^{-1}$ dry weight (or ~4.16 nmol O_2 $min^{-1}mg^{-1}$ dry weight); however kidney respiration was 3-fold higher (Russell, Long, & Wilhelmi, 1944). Oxygen consumption by rat liver acclimated to 30 °C was 6.2 mL O_2 $h^{-1}g^{-1}$, or 4.61 nmol $min^{-1}mg^{-1}$ (Zeisberger, 1966). Oxygen consumption by isolated perfused rat liver was 1.75 nmol $min^{-1}mg^{-1}$; while the rate in isolated hepatocytes was 1.28 ± 0.05 nmol min^{-1} mg^{-1} (Dewar, Bradford, & Thurman, 2002). Thus, the above data show, to some extent, consistency in tissue oxygen consumption despite variabilities in the analytical methods and tissue processing procedures.

In summary, we present a novel method for in vitro measurement of the respiration of murine lung, liver, spleen, kidney and pancreatic tissues over several hours. The procedure is suitable for screening organ toxicity in vitro (Al Shamsi et al., 2010). It is highly sensitive and reproducible. It markedly reduces animal use, since a single organ can be sufficient for all measurements. Moreover, multiple organs from the same animal can be tested at the same time. However, as previously suggested (Lin, Huang, Zhou, & Ma, 2006), this in vitro system needs to be correlated with in vivo testing.

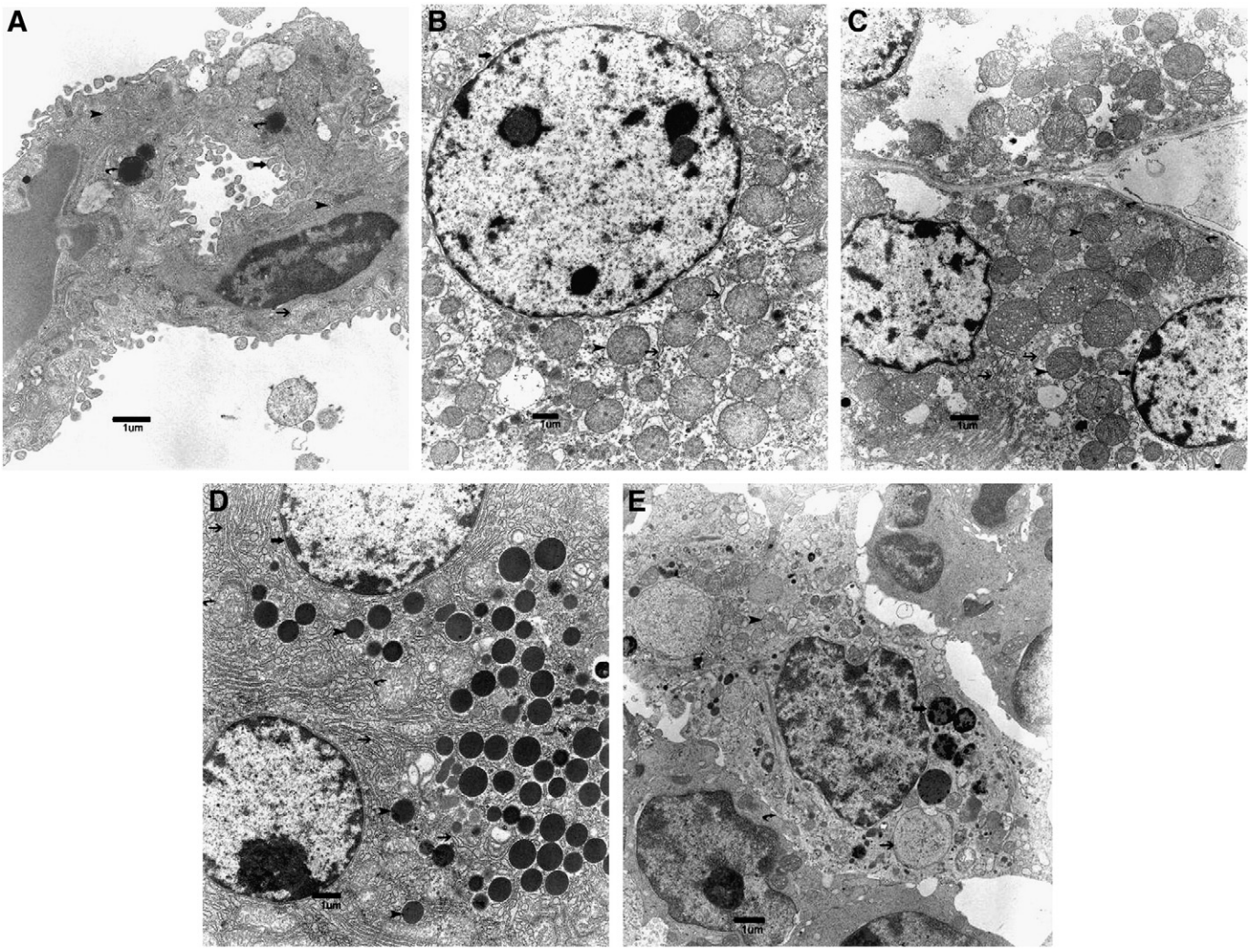

Fig. 4. Transmission electron micrographs showing ultrastructural sections of the studied tissues. (A) Lung tissue showing type 2 pneumocyte with intracytoplasmic lumen containing microvilli (thick arrow). There is preservation of the rough endoplasmic reticulum (arrow heads), membrane-bound dense core vacuoles (curved arrow) and cell membrane (thin arrow). (B) Liver tissue showing preservation of the mitochondria (arrow head), rough endoplasmic reticulum (thin arrow) and nuclear membrane (thick arrow). (C) Renal tissue showing preservation of the mitochondria (arrow head), rough endoplasmic reticulum (thin arrow), cell membrane (curved arrow) and nuclear membrane (thick arrow). (D) Exocrine pancreatic tissue showing preservation of mitochondria (curved arrow), rough endoplasmic reticulum (thin arrow), zymogen granules (arrow head) and nuclear membrane (thick arrow). (E) Splenic tissue showing intra-sinusoidal macrophage and preservation of ultrastructural micro-organelles, including the mitochondria (arrow head), lysosome (thick arrow), vacuole (thin arrow) and cell membrane (curved arrow) of an endothelial cell lining the sinusoidal space.

References

Adler, S., & Huang, H. (2002). Impaired regulation of renal oxygen consumption in spontaneously hypertensive rats. *Journal of the American Society of Nephrology*, *13*, 1788−1794.

Al Shamsi, M., Al Samri, M. T., Al-Salam, S., Conca, W., Shaban, S., Benedict, S., Tariq, S., Biradar, A., Penefsky, H. S., Asefa, T., & Souid, A. -K. (2010). Biocompatibility of calcined mesoporous silica particles with cellular bioenergetics in murine tissues. *Chemical Research in Toxicology*, *23*, 1796−1805.

Bellarosa, D., Ciucci, A., Bullo, A., Nardelli, F., Manzini, S., Maggi, C. A., & Goso, C. (2001). Apoptotic events in a human ovarian cancer cell line exposed to anthracyclines. *The Journal of Pharmacology and Experimental Therapeutics*, *296*, 276−283.

Crosley, A. P., Jr., Castillo, C., & Rowe, G. G. (1961). The relationship of renal oxygen consumption to renal function and weight in individuals with normal and diseased kidneys. *The Journal of Clinical Investigation*, *40*, 836−842.

Davis, K. J., & Doroshow, J. H. (1986). Redox cycling of anthracyclines by cardiac mitochondria. I. Anthracycline radical formation by NADH dehydrogenase. *The Journal of Biological Chemistry*, *261*, 3060−3067.

Deng, A., Miracle, C. M., Suarez, J. M., Lortie, M., Satriano, J., Thomson, S. C., Munger, K. A., & Blantz, R. C. (2005). Oxygen consumption in the kidney: Effects of nitric oxide synthase isoforms and angiotensin II. *Kidney International*, *68*, 723−730.

Dewar, B. J., Bradford, B. U., & Thurman, R. G. (2002). Nicotine increases hepatic oxygen uptake in the isolated perfused rat liver by inhibiting glycolysis. *The Journal of Pharmacology and Experimental Therapeutics*, *301*, 930−937.

Doroshow, J. H. (1983). Effect of anthracyclines antibiotics on oxygen radical formation in rat heart. *Cancer Research*, *43*, 460−472.

Dranger, D., & Lehninger, A. (1982). Sites of inhibition of mitochondrial electron transport in macrophage-injured neoplastic cells. *The Journal of Cell Biology*, *95*, 527−535.

Lin, W., Huang, Y. -w., Zhou, X. -D., & Ma, Y. (2006). In vitro toxicity of silica nanoparticles in human lung cancer cells. *Toxicology and Applied Pharmacology*, *217*, 252−259.

Lo, L. -W., Koch, C. J., & Wilson, D. F. (1996). Calibration of oxygen-dependent quenching of the phosphorescence of Pd-meso-tetra (4-carboxyphenyl) porphine: a phosphor with general application for measuring oxygen concentration in biological systems. *Analytical Biochemistry*, *236*, 153−160.

Ricci, J. -E., Muñoz-Pinedo, C., Fitzgerald, P., Bailly-Maitre, B., Perkins, G. A., Yadava, N., Scheffler, I. E., Ellisman, M. H., & Green, D. R. (2004). Disruption of mitochondrial function during apoptosis is mediated by caspase cleavage of the p75 subunit of complex I of the electron transport chain. *Cell*, *117*, 773−786.

Russell, J. A., Long, C. N., & Wilhelmi, A. E. (1944). Biochemical studies on shock : IV. Oxygen consumption liver kidney tissue rats hemorrhagic shock. *The Journal of Experimental Medicine*, *79*, 23−33.

Shaban, S., Marzouqi, F., Al Mansouri, A., Penefsky, H. S., & Souid, A. -K. (2010). Oxygen measurements via phosphorescence. *Computer Methods and Programs in Biomedicine*, *100*, 265−268.

Souid, A. -K., Penefsky, H. S., Sadowitz, P. D., & Toms, B. (2006). Enhanced cellular respiration in cells exposed to doxorubicin. *Molecular Pharmaceutics*, *3*, 307−321.

Souid, A. K., Tacka, K. A., Galvan, K. A., & Penefsky, H. S. (2003). Immediate effects of anticancer drugs on mitochondrial oxygen consumption. *Biochemical Pharmacology*, *66*, 977−987.

Tao, Z., Ahmad, S. S., Penefsky, H. S., Goodisman, J., & Souid, A. K. (2006). Dactinomycin impairs cellular respiration and reduces accompanying ATP formation. *Molecular Pharmaceutics*, *3*, 762−772.

Tao, Z., Goodisman, J., Penefsky, H. S., & Souid, A. K. (2007). Caspase activation by anticancer drugs: the caspase storm. *Molecular Pharmaceutics*, *4*, 583−595.
Vaupel, P., Fortmeyer, H. P., Runkel, S., & Kallinowski, F. (1987). Blood flow, oxygen consumption, and tissue oxygenation of human breast cancer xenografts in nude rats. *Cancer Research*, *47*, 3496−3503.
Weiss, R. (1970). The solubility of nitrogen, oxygen, and argon in water and seawater. *Deep-Sea Research*, *17*, 721−735.
Zeisberger, E. (1966). Liver oxygen consumption of cold- and warm-acclimated rats and factors regulating liver oxidative metabolism. *Helgoland Marine Research*, *14*, 528−540.
Zunino, F., & Capranico, G. (1990). DNA topoisomerase II as the primary target of anti-tumor anthracyclines. *Anti-Cancer Drug Design*, *5*, 307−317.